Title
PERTURBED ANGULAR CORRELATION OF GAMMA RAYS

Author
Shirley, D.A.

Publication Date
1972-02-01

Submitted to Annual
Review of Physical Chemistry

LBL-667
Preprint

PERTURBED ANGULAR CORRELATION OF GAMMA RAYS

D. A. Shirley and H Haas

February 1972

AEC Contract No. W-7405-eng-48

LBL-667

DISCLAIMER

LBL-667

PERTURBED ANGULAR CORRELATION OF GAMMA RAYS*

D. A. Shirley and H. Haas†

Department of Chemistry and
Lawrence Berkeley Laboratory
University of California
Berkeley, California 94720

February 1972

I. INTRODUCTION

When radiative decay takes place through a three-level system via the successive emission of two photons, an angular correlation may exist between their propagation directions $\vec{k}_1$ and $\vec{k}_2$. For a system in field-free space this correlation depends upon--and contains information about--radiation parameters alone; i.e., spins and transition multipolarities. The angular correlation may be perturbed, however, if the intermediate level of the three-level system can interact with the environment. Studies of perturbed angular correlations (PAC) can yield useful information either about the system itself or about its environment. Many examples could be given illustrating the application of PAC

*Work performed under the auspices of the U. S. Atomic Energy Commission.

†Present Address: Sektor Kernphysik, Hahn-Meitner Institut, Dl Berlin 39, Germany.

in molecular, atomic, nuclear, and even mesic systems. In fact with a little generalization all optical pumping and double resonance experiments could be treated within the same formalism. Such generalization is useful and instructive, but it lies outside the scope of this article, which deals with PAC of gamma quanta emitted in nuclear decay.

Gamma-ray angular correlations have been of interest in nuclear physics for over three decades. In 1940 D. R. Hamilton (1) gave a theoretical description of angular correlations. The first successful experiments were reported by Brady and Deutsch (2) in 1947. Goertzel (3) described perturbed angular correlations in 1946, and H. Frauenfelder, et al. (4) reported the observation of perturbations in 1951. Comprehensive theoretical descriptions of perturbed angular correlations were presented in 1953 by Alder, et al. (5), and by Abragam and Pound (6), among others. Many other workers contributed to the development of perturbed angular correlations in this period. In the years that followed, nuclear physicists applied this method widely to the determination of nuclear magnetic dipole moments. Frauenfelder and Steffen gave a detailed discussion of the development of the field in their extensive review article (7) published in 1965.

Their article also contains a thorough and lucid description of the theory of perturbed angular correlations. The present review takes as a theoretical basis the formalism given by Frauenfelder and Steffen, and the reader is referred to their article both as the major reference for theoretical derivations and for a bibliography of the literature prior to 1965. Perturbed angular correlations have not been reviewed before in this series. Therefore, the theory is presented below, in two parts. First, an intuitive description is given in which the physical principles of angular correlations are stressed. Next, a brief sketch is given of the general theory of PAC using the density matrix-perturbation coefficient formalism. In the past seven years a number of significant advances have been made in the applications of perturbed angular correlations to the study of extranuclear properties. These advances are reviewed in Section III, with emphasis on topics of interest in physical chemistry.

An outline is given below for reference.

II. ANGULAR CORRELATION THEORY

A. A "Physical" Approach

In this subsection a simple, but exact, theory of angular correlations is given, using concepts that are familiar from atomic spectroscopy and magnetic resonance. The object of Section II.A.1 is to establish the origins of the angular correlation phenomenon, and in Section II.A.2 it is shown how oscillatory modulation follows from magnetic perturbations.

1. Unperturbed Angular Correlations.--

Unperturbed angular correlation phenomena can be described very simply in terms of substate populations. Consider the γ-γ cascade

$$I_i \xrightarrow{\gamma_1(L')} I \xrightarrow{\gamma_2(L)} I_f$$

in which an initial nuclear state of spin I_i emits a (γ_1) quantum of multipolarity L', forming an intermediate state of spin I that subsequently decays via emission of a (γ_2) quantum to the final state, of spin I_f. The two γ quanta are sensed with separate detectors, and the coincidence counting rate, $W(\Theta)$, is recorded as a function of the angle Θ between the propagation vectors

$\vec{k}_1$ and $\vec{k}_2$ of the two γ quanta, as shown in Figure 1. We wish to work out an expression for $W(\theta)$.

First we observe that in the initial state $|I_i\rangle$ the nuclear spins are randomly oriented. This can be stated formally by writing

$$\rho^{(i)}_{m_i m_i'} = \delta_{m_i m_i'} (2I_i + 1)^{-1} \qquad 1.$$

where $\rho^{(i)}_{m_i m_i'}$ is an element of the density matrix that describes magnetic substate populations of the initial state $|I_i\rangle$ in any m representation. Now we seek an expression for the density-matrix elements describing the substate populations of the intermediate state $|I\rangle$ immediately after the emission of γ_1. From angular-momentum theory we know that when a magnetic substate $|I_i m_i\rangle$ decays to the substates $|Im\rangle$ of state $|I\rangle$, the fractional intensity decaying to each substate $|Im\rangle$ is given by the square of the Clebsch-Gordan coefficient $\langle I\ m\ L'(m_i - m)|I_i m_i\rangle$. Up to this point the quantization direction is arbitrary, although it must be the same for the two states $|I_i\rangle$ and $|I\rangle$. To take full advantage of the cylindrical symmetry of the system about the $\vec{k}_1$ direction, however, let us select the quantization axis as being along $\vec{k}_1$. Having made this choice, we must assign to each individual component of the γ_1 transition

a weighting factor $\omega(mm')$, which is the ratio of the probability of photon emission in the $\vec{k}_1$ direction to the average probability of emission in any direction. This is done by noting that for a transition of multipolarity L', between states having magnetic quantum numbers m and m_i, the photon angular distribution has the form

$$W^{(L'M')}(\Theta) = \sum_{\lambda' \text{even}} a_{\lambda'L'M'} P_{\lambda'}(\cos\Theta) \quad , \qquad 2.$$

where $M' = m_i - m$ and Θ is the polar angle from the quantization axis. Both λ' and L' must satisfy triangle conditions (8), but $W^{(L'M')}(\Theta)$ is otherwise independent of the spins I and I_i. The coefficients $a_{\lambda'L'M'}$ can be evaluated by comparison of Equation (2) with the well-known (9) angular distribution functions $W^{(11)}(\Theta) \propto 1 + \cos^2\Theta$, $W^{(10)}(\Theta) \propto \sin^2\Theta$, etc. Values of $a_{\lambda'L'M'}$ for dipole and quadrupole radiation are given in Table 1. By normalization, $a_{0L'M'} \equiv 1$ for all L' and M'. Now we note that

$$\omega(mm_i) = \frac{W^{(L'M')}(0)}{(W^{(L'M')})_{AV}} = \sum_{\lambda'} a_{\lambda'L'M'} \quad . \qquad 3.$$

Thus the required intermediate-state density-matrix elements are given at the time of formation of the intermediate state ($t = 0$) by

Table 1. Coefficients of $P_2(x) = \frac{3}{2}x^2 - \frac{1}{2}$ and $P_4(x) = \frac{35}{8}x^4 - \frac{15}{4}x^2 + \frac{3}{8}$ for for Dipole and Quadrupole Radiation (Eq. (2))[a]

L'	M'	$a_{2L'M'}$	$a_{4L'M'}$
1	0	-1	--
1	±1	1/2	--
2	0	5/7	-12/7
2	±1	5/14	8/7
2	±2	-5/7	-2/7

[a] Normalized to $a_{0L'M'} = 1$ for all L' and M'.

$$\rho_{mm}(t = 0) = (2I_i + 1)^{-1} \sum_{m_i} \langle I\ m\ L'M' | I_i m_i \rangle^2 \sum_{\lambda'} \left[a_{\lambda' L' M'} \right] \quad . \qquad 4.$$

To complete the calculation of $W(\Theta)$, we now consider the individual components of the second transition. Each component proceeds from a substate $|Im\rangle$ to a substate $|I_f m_f\rangle$ of the final state via emission of a gamma quantum of multipolarity L having magnetic component $M = m - m_f$ relative to the $\vec{k}_1$ axis. Each component has an angular distribution relative to $\vec{k}_1$ of

$$W^{(LM)}(\Theta) = \sum_{\lambda \text{ even}} a_{\lambda LM} P_\lambda(\cos \Theta) \quad . \qquad 2'.$$

Summing over components, we have

$$W(\Theta, t) = \sum_{m_f} \sum_{m} \rho_{mm}(t)\ W^{(LM)}(\Theta) \langle I_f m_f L\ M | Im \rangle^2 \quad . \qquad 5.$$

Here time-dependence has been explicitly introduced in the density matrix to allow for its time evolution in the intermediate state. After changing the order of summation, invoking the summation properties of the Clebsch-Gordan coefficients, and noting that decay of the intermediate state gives $\rho_{mm}(t) = \rho_{mm}(0)\ e^{-t/\tau}$, where τ is the intermediate-state lifetime, Equation (5) becomes

$$W(\Theta,t) = e^{-t/\tau}\left[1 + \sum_{\lambda=2,4,\ldots} C_\lambda P_\lambda(\cos\Theta)\right] . \qquad 6.$$

The coefficients C_λ are given by

$$C_\lambda = (2I_i + 1)^{-1} \sum_{m_f m m_i} a_{\lambda LM} \langle I_f m_f LM | Im \rangle^2 \langle Im\, L'M' | I_i m_i \rangle^2 \sum_{\lambda'=0,2,4\ldots} a_{\lambda' L' M'} . \qquad 7.$$

They may be calculated from Table 1 and the appropriate Clebsch-Gordan coefficients. Values of C_λ for a few selected spin sequences are given in Table 2.

The above results were derived for transitions of pure multipolarities. It is straightforward, but tedious, to extend this approach to mixed-multipolarity transitions. Such transitions are, however, easily treated using the more general theory discussed in Section II.B.

2. Perturbation by a Magnetic Field.--

If extranuclear fields are present during an angular correlation experiment, they will interact with the nuclear moments of the intermediate state. This perturbation may coherently mix the magnetic substates and affect the angular-correlation pattern. The general theory of perturbed angular correlations, which is useful for describing this phenomenon, is somewhat formidable

Table 2. Coefficients C_λ for Selected Cascades

Spin Sequence[a]	C_2	C_4
0(D) 1(D) 0	0.5000	0
0(Q) 2(Q) 0	0.3574	1.1428
4(Q) 2(Q) 0	0.1020	0.0091
1(D) 2(D) 1	0.1750	0
1(Q) 2(Q) 1	0.0893	0.5079
$\frac{3}{2}$(D) $\frac{5}{2}$(Q) $\frac{5}{2}$	0.0714	0
$\frac{7}{2}$(Q) $\frac{3}{2}$(D) $\frac{5}{2}$	-0.0143	0

[a] D = dipole, Q = quadrupole. Directional correlations are insensitive to parity: thus electric and magnetic dipole radiation may be treated equivalently. Also, C_2 and C_4 are unchanged if the entire spin sequence is reversed.

on first encounter. For this reason we consider below the important special case of the interaction between a nuclear magnetic moment and a magnetic field, using as a theoretical framework the simple torque equation-rotating frame description familiar from NMR theory. This approach shows how Larmor precession leads naturally to oscillations, or "quantum beats", in the angular correlation function.

Consider an angular-correlation experiment conducted in the presence of a magnetic field $\vec{H}$, and suppose that $\vec{k}_1$, $\vec{k}_2$, and $\vec{H}$ have arbitrary orientations relative to one another. We may, without loss of generality, select a laboratory coordinate frame such that the z direction is along $\vec{H}$ and $\vec{k}_2$ is in the xz plane. Thus $\phi_2 = 0$, while θ_1, ϕ_1, and θ_2 are arbitrary, as shown in Figure 2.

The dynamical behavior of a system with magnetic moment $\vec{M}$ in a field $\vec{H}$ is governed by the torque equation

$$\frac{d\vec{M}}{dt} = \frac{g\mu_N}{\hbar} \vec{M} \times \vec{H} \quad . \qquad 8.$$

Thus $\vec{M}$ precesses about $\vec{H}$ with angular frequency $\omega_L = -\frac{g\mu_N H}{\hbar}$. Now Larmor's Theorem states that the system's dynamical behavior in a coordinate frame rotating about $\vec{H}$ with angular frequency ω_L is equivalent to its behavior in

the laboratory frame with no magnetic field present. A transformation into this rotating frame therefore greatly simplifies the study of a magnetic system's dynamical behavior. The magnetically-perturbed angular correlation experiment can be treated in a similar way. A simplifying feature of unperturbed angular correlations is the time-independence (except for the multiplicative factor $e^{-t/\tau}$) of the density matrix in an m representation with $\vec{k}_1$ as the symmetry direction. This feature is lost when the system is perturbed by a magnetic field, and it is desirable to restore it. This can be accomplished by defining a vector $\vec{K}(t)$ that evolves according to the generalized torque equation (10)

$$\frac{d\vec{K}}{dt} = \frac{g\mu_n}{\hbar} \vec{K} \times \vec{H} \quad , \qquad 9.$$

subject to the initial condition $\vec{K}(t = 0) = \vec{k}_1$. This equation is completely equivalent to the torque equation, but it doesn't require that $\vec{M}$ be nonzero. Because the density matrix $\tilde{\rho}$ was diagonal in an $|Im\rangle$ representation along $\vec{k}_1$ at t = 0, it follows from Larmor's Theorem that $\tilde{\rho}(t)$ will retain its diagonal character along $\vec{K}(t)$. The time-dependent perturbed angular correlation function in the presence of a magnetic field can then be written (cf. Equation (6)) as

$$W[\Theta(t),t] = e^{-t/\tau}\left\{1 + \sum_{\lambda=2,4} C_\lambda\, P_\lambda[\cos\,\Theta(t)]\right\} \quad , \qquad 10.$$

where the time-dependent angle between $\vec{K}(t)$ and $\vec{k}_2$ obeys the cosine law (see Figure 2)

$$\cos\,\Theta(t) = \cos\,\theta_1\,\cos\,\theta_2 + \sin\,\theta_1\,\sin\,\theta_2\,\cos(\omega_L t + \phi_1) \quad . \qquad 11.$$

It is instructive to derive the functions describing the oscillatory modulation of the angular correlation pattern, arising from Larmor precession, in several commonly-used geometrical orientations of $\vec{H}$, $\vec{k}_1$, and $\vec{k}_2$. This may be done by assigning the appropriate values to θ_1, θ_2, and ϕ_1, and combining Equations (10) and (11). First let us take $\vec{H}$ parallel to $\vec{k}_1$ or $\vec{k}_2$ by setting either θ_1 or θ_2 equal to zero. Equation (11) then gives

$$\begin{aligned} \cos\,\Theta &= \cos\,\theta_2 \qquad \text{if } \theta_1 = 0 \\ &= \cos\,\theta_1 \qquad \text{if } \theta_2 = 0 \quad . \end{aligned} \qquad 12.$$

In either case Θ is time-independent and Equation (10) reduces to Equation (6). Thus we have the well-known result that a geometry with $\vec{H}$ parallel to $\vec{k}_1$ or $\vec{k}_2$ gives the unperturbed correlation.

In "perpendicular" geometry, with $\theta_1 = \theta_2 = \pi/2$, we have $\cos\Theta = \cos(\phi_1 + \omega_L t)$. Substitution into Equation (10) gives

$$W[\Theta(t),t] = e^{-t/\tau}\left\{1 + \sum_{\lambda=2,4\ldots} C_\lambda P_\lambda[\cos(\phi_1 + \omega_L t)]\right\} \quad . \qquad 13.$$

Because $\Theta(t = 0) = \phi_1$ for this geometry, comparison with Equation (6) shows that application of a magnetic field perpendicular to the correlation plane has the effect of replacing the angle Θ between $\vec{k}_1$ and $\vec{k}_2$ by $\Theta + \omega_L t$. Larmor precession may be observed directly, through oscillations of frequency $2\omega_L$ and higher in $W[\Theta(t),t]$. This allows measurement of nuclear moments and Knight shifts by time-differential perturbation.

R. S. Raghavan et al. (11) have recently pointed out two geometries that emphasize oscillations of frequency ω_L, rather than $2\omega_L$, when $\lambda = 2$. In our notation these geometries may be described as $A(\theta_1 = \theta_2 = \frac{\pi}{4})$ and $B(\theta_1 = \frac{\pi}{4}, \theta_2 = \frac{3\pi}{4})$, with $\phi_1 = \pi$ in each case. Thus

$$\cos\Theta(t) = -\frac{1}{2}(\cos\omega_L t \mp 1) \quad , \qquad 14.$$

where the - sign applies to Geometry A and the + sign to Geometry B. Substitution into Equation (10) yields

$$W_{A,B}[\Theta(t),t] = e^{-t/\tau} \{1 + \frac{C_2}{16} [1 + 3 \cos 2\omega_L t \mp 12 \cos \omega_L t]\} \quad . \qquad 15.$$

The difference $W_A - W_B$ shows oscillations of frequency $\omega_L t$ only, in agreement with Reference 11.

In the "random fields" geometry (12), which applies in PAC studies of unmagnetized ferromagnets, the relative angles $\theta_2 + \theta_1 = \pi$ and $\phi_2 - \phi_1 = \pi$ are fixed, but θ_1 is random. Substituting into Equations (10) and (11), truncating at $\lambda = 2$, and averaging over θ_1 ($\overline{\cos^n \theta_1} = 1/(n + 1)$, for even n), we find

$$W(t) = \frac{1}{5} [1 + 2 \cos \omega_L t + 2 \cos 2\omega_L t] \quad , \qquad 16.$$

showing that random-fields geometry yields equal-amplitude oscillations at frequencies ω_L and $2\omega_L$.

Figure 3 shows experimental curves obtained with a sample of ^{100}Rh in a Cu lattice in an external magnetic field. Oscillations arising from Larmor precession are clearly visible.

B. The General Theory of Perturbed Angular Correlations

Many workers have contributed to the development of PAC theory. A detailed derivation of the important results, together with reference to the

original literature, is given in the comprehensive review article by Frauenfelder and Steffen (7). A brief outline of the theory is given below. It follows the Frauenfelder-Steffen treatment closely in the main, differing in notation and in the specific use of the density matrix formalism (13).

The process to be described is the γ-γ cascade in which an initial nuclear state evolves into a final nuclear state under the sequential influence of three interactions. These interactions are: emission of γ_1, perturbation of the intermediate state by extranuclear fields, and emission of γ_2. The first and last steps are governed by the transition Hamiltonians $\mathcal{H}^{(1)}$ and $\mathcal{H}^{(2)}$, respectively, while the intermediate-state perturbation is described by a time-evolution operator $\Lambda(t)$. From first-order perturbation theory we have

$$W(k_1,k_2,t) \propto \sum_{i,f} |\langle f|\mathcal{H}^{(2)}\Lambda(t)\mathcal{H}^{(1)}|i\rangle|^2 \quad . \qquad 17.$$

The sums are taken over any complete sets of basis functions that span the initial and final states. The labels $\vec{k}_1$, $\vec{k}_2$, and t in W indicate that the derivation should lead to an expression of sufficient generality that these three quantities are left as variable arguments. Expansion of Equation (17) gives

$$W(\vec{k}_1,\vec{k}_2,t) \propto \sum_{i,f,a,\bar{a},b,\bar{b}} \mathcal{H}^{(2)}_{fb}\, \Lambda(t)_{ba}\, \mathcal{H}^{(1)}_{ai}\, \mathcal{H}^{(2)*}_{f\bar{b}}\, \Lambda(t)^{*}_{\bar{b}\bar{a}}\, \mathcal{H}^{(1)*}_{\bar{a}i} \quad , \qquad 18.$$

where a, b, $\bar{a}$, and $\bar{b}$ label a complete set of substates spanning the intermediate nuclear state. The sums may be rearranged into the form

$$W(\vec{k}_1,\vec{k}_2,t) = \sum_{a,\bar{a},b,\bar{b}} \left(\sum_i \mathcal{H}^{(1)}_{ia}\, \mathcal{H}^{(1)*}_{i\bar{a}} \right) \left(\Lambda_{ba}(t)\, \Lambda_{\bar{b}\bar{a}}(t)^{*} \right) \left(\sum_f \mathcal{H}^{(2)}_{bf}\, \mathcal{H}^{(2)*}_{\bar{b}f} \right) \quad , \quad 19.$$

separating the three factors that can be associated with the γ_1 transition, the γ_2 transition, and the intermediate-state perturbation, which is connected by <u>two</u> indices to each of the other two factors.

The time-evolution operator $\Lambda(t)$ obeys the Schrödinger Equation. It can be expressed in terms of the intermediate-state Hamiltonian K as

$$\Lambda(t) = \exp\left(-\frac{i}{\hbar} \int_0^t K(t')dt' \right) \quad . \qquad 20.$$

If K is time-independent, the argument of the exponential reduces to $-(\frac{i}{\hbar})Kt$. We may also describe unperturbed angular correlations, starting from Equation (19). For this case, K = 0 and Λ = 1. Thus

$$\Lambda_{ab}(t) = \delta_{ab}$$

$$\Lambda_{\bar{a}\bar{b}}(t) = \delta_{\bar{a}\bar{b}} \qquad 21.$$

for the unperturbed case. Two indices suffice to describe the intermediate level, and no mixture of substates is implied. In general, however, $\Lambda \neq 1$, and all four indices a, $\bar{a}$, b, $\bar{b}$ must be retained.

It is convenient to describe perturbed angular correlations in a spherical-tensor basis. The summation indices in Equation (19) can then be taken as the tensor ranks λ and λ', together with their components q and q' (where, e.g., $q = \lambda, \lambda-1, \ldots -\lambda$) describing the two transitions. After some algebra Equation (19) becomes

$$W(\vec{k}_1,\vec{k}_2,t) = \sum_{\lambda\lambda' qq'} [(2\lambda' + 1)^{-1/2} A_{\lambda'}(1) Y_{\lambda'}^{q'*}(\theta_1,\phi_1)] G_{\lambda',\lambda}^{q'q}(t)$$

$$\times [(2\lambda + 1)^{-1/2} A_{\lambda}(2) Y_{\lambda}^{q}(\theta_2,\phi_2)] \quad . \qquad 22.$$

The first and third factors depend on the experimental geometry and the radiation parameters of the λ transitions. The <u>perturbation factor</u> $G_{\lambda',\lambda}^{q'q}(t)$ carries all the information about interactions of the intermediate state with the extra-nuclear environment.

Before examining $G_{\lambda',\lambda}^{q'q}(t)$ in detail, let us discuss the radiation parameters $A_{\lambda'}(1)$ and $A_{\lambda}(2)$. These parameters are independent of intermediate-state perturbations. They depend only upon the multipolarities and spins of the two transitions. The theory of (unperturbed) angular correlations provides these radiation parameters. It has been formulated with sufficient generality to deal with arbitrary spins and multipolarities. Each transition is allowed either to be pure or to be a mixture of two multipolarities. Thus cascades of the form

$$I_i \xrightarrow{\gamma_1(L_1,L_1')} I \xrightarrow{\gamma_2(L_2,L_2')} I_f$$

can be treated. Each transition has associated with it a set of F coefficients defined (14) (for the first transition) by

$$F_{\lambda'}(L_1L_1'I_iI) = (-1)^{I_i-I-1}[(2L_1+1)(2L_1'+1)(2I+1)]^{1/2}$$

$$\times \langle L_1 1\, L_1' - 1 | \lambda' 0 \rangle W(II\, L_1L_1';\lambda' I_i) \quad , \qquad 23.$$

where $W(II\, L_1L_1';\lambda' I_i)$ is a Racah coefficient. The coefficients $F_{\lambda'}(L_2L_2'I_fI)$ for the second transition are given by Equation (23), but with the subscripts

i and 1 replaced by f and 2, respectively. The C_λ coefficients in Equation (6) are then given by

$$C_\lambda = A_\lambda^{(1)} A_\lambda^{(2)} \qquad 24.$$

where

$$A_\lambda^{(1)} = \frac{F_\lambda(L_1 L_1 I_i I) + (-1)^{L_1+L_1'} 2\delta_1 F_\lambda(L_1 L_1' I_i I) + \delta_1^2 F_\lambda(L_1' L_1' I_i I)}{1 + \delta_1^2} \qquad 25.$$

and similarly for $A_\lambda^{(2)}$. In this expression δ_1 is the ratio of the reduced matrix elements for multipolarities L_1' and L_1, defined by

$$\delta_1 = \langle I \| \vec{j}_N \vec{A}_{L_1'} \| I_i \rangle / \langle I \| \vec{j}_N \vec{A}_{L_1} \| I_i \rangle \quad . \qquad 26.$$

Here the matrix elements are written in terms of the nuclear current and vector-potential operators. Nuclear-structure theories can predict δ values with low accuracy only, and empirical determinations of δ are desirable. When the angular correlation is perturbed, it is not always possible to reduce the general form for $W(\vec{k}_1, \vec{k}_2, t)$ given by Equation (22) to the simple form of Equation (6). The perturbation factor $G_{\lambda',\lambda}^{q'q}(t)$ may be non-zero for $\lambda' \neq \lambda$, and products of the form $A_{\lambda'}^{(1)} A_\lambda^{(2)}$ can occur.

Several numerical tabulations of F-coefficients exist. A few values are presented in Table 3. It should be noted that the C_λ coefficients in Table 2 can be obtained as combinations of F coefficients. Thus for the cascade 4(Q)2(Q)0, we have

$$C_2 = F_2(2\ 2\ 4\ 2)F_2(2\ 2\ 0\ 2) = \left(-\frac{1}{7}\sqrt{\frac{10}{7}}\right)\left(-\sqrt{\frac{5}{14}}\right) = \frac{5}{49}$$

$$C_4 = F_4(2\ 2\ 4\ 2)F_4(2\ 2\ 0\ 2) = \left(-\frac{1}{63}\sqrt{\frac{2}{7}}\right)\left(-2\sqrt{\frac{2}{7}}\right) = \frac{4}{441} \qquad 27.$$

Let us return to the perturbation factor. If the indices a, $\bar{a}$, b, $\bar{b}$ in Equation (19) are taken as magnetic quantum numbers in the intermediate state, then $G^{q'q}_{\lambda'\lambda}(t)$ has the form (7)

$$G^{q'q}_{\lambda'\lambda}(t) = \sum_{a,b} (-1)^{2I+a+b}\,[(2\lambda+1)(2\lambda'+1)]^{1/2} \begin{pmatrix} I & I & \lambda' \\ \bar{a} & -a & q' \end{pmatrix} \begin{pmatrix} I & I & \lambda \\ \bar{b} & -b & q \end{pmatrix} \Lambda(t)_{ba}\Lambda(t)^{*}_{\bar{b}\bar{a}} \,. \qquad 28.$$

The factors in Equation (22) are arranged to emphasize the symmetry of the angular correlation. In many PAC problems, however, it is valuable to stress the evolution of the intermediate state in time. We define statistical tensors (13)

Table 3. Selected values of F-coefficients[a]

I	I'	$F_2(11I'I)$	$F_2(22I'I)$	$F_4(22I'I)$
1	0	0.7071	--	--
2	0	--	-0.5978	-1.0690
2	1	0.4183	-0.2988	0.7127
2	2	-0.4183	0.1281	-0.3054
2	3	0.1195	0.3415	0.0764
2	4	--	-0.1707	-0.0085
3/2	1/2	0.5000	-0.5000	--
3/2	5/2	0.1000	0.3571	--
3/2	7/2	--	-0.1429	--
5/2	1/2	--	-0.5345	-0.6172
5/2	3/2	0.3742	-0.1909	0.7054
5/2	5/2	-0.4276	0.1909	-0.3968
5/2	7/2	0.1336	0.3245	0.1176

[a] From M. Ferentz and N. Rosenzweig, Argonne National Laboratory Report ANL-5324, 1957 (unpublished). Blanks indicate cases that vanish by triangle conditions.

$$\rho_{q}^{\lambda'}(t = 0) = \sum_{a} (-1)^{I+a} \langle I-a\ I\bar{a} | \lambda' q' \rangle \rho_{a\bar{a}} \qquad 29.$$

where $\rho_{a\bar{a}}$ is an element of the density matrix describing the intermediate state at the instant of its formation, $t = 0$. It can be shown (13) that

$$W(\vec{k}_1,\vec{k}_2,t) = \frac{4\pi e^{-t/\tau}}{\tau} \sum_{\lambda\lambda' qq'} [(2\lambda + 1)(2\lambda' + 1)]^{-1/2} \rho_0^{\lambda'}(0)_{\vec{k}_1} A_\lambda(2) G_{\lambda',\lambda}^{q',q}(t) Y_{\lambda' q'}(\theta_1,\phi_1)^*$$

$$\times Y_{\lambda q}(\theta_2,\phi_2) \quad . \qquad 30.$$

Here the subscript $\vec{k}_1$ denotes that the statistical tensors $\rho_{q'}^{\lambda'}$ are evaluated at $t = 0$ in the $\vec{k}_1$ frame, wherein they are nonzero only if $q' = 0$. The actual values of $\rho_0^{\lambda}(0)$ depend on the radiation parameters $A_{\lambda'}(1)$ of γ_1. The factor $[4\pi/(2\lambda' + 1)]^{1/2}\ Y_{\lambda'}^{q'}(\theta_1,\phi_1)^*$ arises from a transformation into the frame in which $G_{\lambda',\lambda}^{q',q}(t)$ is expressed. The factor $\tau^{-1}\exp(-t/\tau)\ G_{\lambda',\lambda}^{q',q}(t)$ represents evolution and decay of the intermediate state in this frame, and the factor $[4\pi/(2\lambda + 1)]^{1/2}\ Y_{\lambda}^{q}(\theta_2,\phi_2)$ arises from a transformation into the k_2 frame. By starting from the von Neumann equation

$$i\hbar\dot{\rho} = [K,\rho] \quad , \qquad 31.$$

with both the density matrix ρ and the Hamiltonian K expressed in the same frame as $G^{q'q}_{\lambda'\lambda}(t)$, it is straightforward to show that

$$\rho^{\lambda}_{q}(t) = \sum_{\lambda' q'} G^{q'q}_{\lambda'\lambda}(t)^{*}\ \rho^{\lambda'}_{q'}(0) \quad . \tag{32.}$$

That is, the perturbation factors are expansion coefficients describing the time-development of the statistical tensors.

In most cases the full generality of the theory given above is not required. If $G^{q'q}_{\lambda'\lambda}(t)$ is expressed in a representation in which K is diagonal, then only terms with $q = q'$ are nonzero. Often $\lambda_{max} = 2$. In this case only a single time-dependent perturbation factor survives, and the correlation may be written

$$W(\vec{k}_1,\vec{k}_2,t) = \frac{4\pi e^{-t/\tau}}{\tau}\,[1 + C_2 G_{22}(t)\ P_2(\cos\theta)] \quad , \tag{33.}$$

where $C_2 = A_2(1)\ A_2(2)$. This may be compared with Equation (6). At $t = 0$ $G_{22}(0) = 1$ and the unperturbed correlation is obtained.

It is usually feasible to select the angles $\theta_1\phi_1\theta_2\phi_2$ in a way that facilitates extraction of the perturbation factors from the data. Thus only

these factors need be considered. We shall assume that this is the case in the following discussion.

III. THE EXPERIMENTAL SITUATION

The foregoing theoretical treatment was worked out in principle in the early 1950's. It gives a description of what could be observed under ideal conditions. Even as recently as 1965 this elegant and complete theory stood in sharp contrast to a relatively crude experimental situation. The reason for this difference is simple. Most γ-ray angular correlation cascades are preceded by one of the forms of beta decay, with accompanying elemental transmutation. This process can so disrupt the extranuclear environment in the daughter as to obviate observing a well-defined angular correlation (15). Much of the recent progress on the experimental side in PAC has been based on understanding the conditions under which problems associated with elemental transmutation can be avoided. A logical approach to this question, and in fact to a general discussion of experimental progress in PAC, must involve consideration of three factors:

1. The nature of the sample.
2. The mode of preceding decay.
3. The type of intermediate-state interaction.

Several qualitatively different categories can be specified under each of these headings. While the actual number is somewhat arbitrary, four such categories will suffice to cover the range of phenomena encountered in each case. Accordingly, we have chosen to classify PAC experiments in "boxes" as shown in Figure 4. Each box is described by three coordinates, corresponding to "values" of the factors listed above. These triads will be used to label portions of the discussion below. The 64 boxes are treated in greatly different detail, commensurate with their relative importance in recent years. Thus some boxes or $1 \times 1 \times 4$ "rows" will be accorded as much space as other whole $4 \times 4 \times 1$ "layers".

A. Angular Correlations in Metals

The strongly reducing atmosphere provided by conduction electrons makes a metallic lattice an ideal environment for PAC experiments. In a disruptive nuclear event such as beta decay the daughter atom may lose electrons and be placed in a highly-oxidized state. The daughter nucleus is also in an excited "initial" state preceding the correlation cascade. Since the electron correlation time in a metal is of the order of 10^{-12} sec, or appreciably shorter

than the nuclear initial-state lifetime of 10^{-10} - 10^{-11} sec in most cases, the electronic configuration usually recovers before the emission of the γ_1 photon. Even if the initial state lifetime is shorter than the electron correlation time, the influence of the fast electronic fluctuations on the nuclear alignment present after the first γ-event can usually be neglected. Thus for most studies in metals disruptive chemical effects can be ignored. Provided that the probability of recoil into an interstitial site may also be neglected, the four modes of decay indicated in Figure 1 can be considered together in discussing PAC experiments in metals.

1. Magnetic Interactions in Metals.--

During the 1960's the measurement of Larmor frequencies evolved from studies of nuclear g factors with 5-10% accuracy up to a level at which Knight shifts in metals could be measured, with the limiting factor being the natural width of the intermediate nuclear state. This improvement can be attributed mainly to the advent of time-differential PAC (16,17) and to the use of metallic lattices (18). A useful modification of data analysis is the Fourier transformation of the correlation function $W(\theta,t)$ into the frequency domain, where it can be studied as an NMR line would be (19). Starting with Equation (13), and specializing it to the case of $C_\lambda = 0$ for $\lambda > 2$, we can rewrite P_2 to give, for an angle $\phi_1 = \pi$ between $\vec{k}_1$ and $\vec{k}_2$,

$$W(\pi,t) = \left[1 + \frac{C_2}{4} + \frac{3C_2}{4}\cos 2\omega_L t\right] e^{-t/\tau} \quad . \qquad 34.$$

A Fourier cosine transform yields

$$F(\omega) = \frac{1}{2\pi}\int_{-\infty}^{\infty} W(\pi,t)\cos\omega t\, dt \cong \frac{3C_2\tau}{8\pi}\left[1 + (2\omega_L - \omega)^2\tau^2\right]^{-1} \quad , \quad 35.$$

where only the "resonant" branch, with ω having the same sign as ω_L, has been retained. Here $F(\omega)$ is a Lorentzian, of half width $\Delta\omega$ at half maximum equal to τ^{-1}. It can be regarded as a free precession version of an NMR line, with no radiofrequency field. For ^{100}Rh, $F(\omega)$ functions with close to the natural linewidth have been observed (20). In some cases autocorrelation functions with enhanced signal-to-noise ratio were generated prior to the Fourier transformation (19,20).

The higher-precision frequency determinations in metals has made possible a number of measurements that are not feasible using conventional methods. For example, Alonso and Grodzins (21) used PAC in ^{100}Rh to study flux distribution in type-II superconductors. With PAC they could study this property in static fields only, without the fluxoid motion that would be

incurred by the radiofrequency fields required in NMR studies. In another case, Rao et al. (20) studied the strongly temperature-dependent Knight shifts of ^{100}Rh in very dilute solutions in Pd lattices. They found that the local susceptibility on the Rh atoms continues to increase as the temperature is lowered, in contrast to the lattice susceptibility and Knight shift, which decrease below 80°K. This study would not be possible at such dilutions using NMR, because the sensitivity of NMR is several orders of magnitude lower.

Hyperfine fields in ferromagnets have been studied extensively by PAC methods. The advantage of PAC over NMR or Mössbauer spectroscopy for these studies lies in its high sensitivity and applicability at all temperatures. Thus it is especially suited for measuring the temperature dependence of hyperfine fields of solutes in ferromagnets. Such measurements can help to establish the extent of localized magnetism on impurities. For example, PAC experiments on ^{111}Cd and ^{99}Ru in a nickel lattice established that ^{99}Ru has a localized magnetic moment, while the ^{111}Cd hyperfine field follows the lattice (22) magnetization. In the ^{111}Cd<u>Ni</u> case it was possible to predict very large paramagnetic shifts above the Curie point, T_c, from the temperature dependence

of H_{hf} below T_c. To a good approximation the cadmium hyperfine field at temperature T below T_c could be described by

$$H_{hf}(Cd,T) = H_{hf}(Cd,0)\,\frac{\sigma(T)}{\sigma(0)} \quad , \qquad 36.$$

where $\sigma(T)$ is the lattice magnetization of nickel at temperature T. If $H_{hf}(Cd)$ arises only from conduction-electron polarization, a similar relation should hold above the Curie point. Thus in an applied field H the effective field at the ^{111}Cd nucleus should be

$$H_{eff} = \beta H = 1 + \frac{H_{hf}(Cd,0)}{H}\,\frac{\sigma(T,H)}{\sigma(0,H)} \quad . \qquad 37.$$

Values of β predicted from this relation were in fact found to agree very well with experiment. A comparison is shown in Figure 5.

Reno and Hohenemser (23) reported a very elegant application of PAC to a study of collective properties. They measured H_{hf} of ^{100}Rh in nickel to very high precision close to T_c, finding that the critical exponent β that appears in the expression

$$H_{hf} \propto [1 - T/T_c]^{\beta} \qquad 38.$$

has the value $\beta = 0.385 \pm 0.005$ for the range $10^{-1} > (1 - T/T_c) > 10^{-4}$. This result is in agreement with measurements of β in nickel based on other properties, but the accuracy of this determination is unusually good.

2. Quadrupole Interactions in Metals.--

Although time-differential PAC spectra showing quadrupole interactions in metals were obtained as early as 1955 by Lehmann and Miller (24), only relatively few results have been reported to date. Recent work by R. S. Raghavan on ^{111}Cd in Cd metal (25) and ^{117}In in In metal (26) as well as studies by the reviewers on a total of thirty combinations of solute nuclei in metallic host lattices (27) have now shown that high-precision studies of quadrupole frequencies in metals are possible using PAC methods. Two results of the latter study are: (1) In favorable cases many cycles of oscillation were observed, with no apparent attenuation in the amplitude of the oscillations, and (2) For the especially important hcp lattices the magnitudes of the observed field gradients are directly related to the deviation of the host-lattice c/a ratio from the ideal value of 1.6. Thus the quadrupole coupling constants of solutes in Mg and Tl, which have $c/a \cong 1.6$ tend to be small, while

in Zn(c/a = 1.86), and especially in Cd(c/a = 1.89), the coupling constants are relatively large. Representative quadrupole coupling constants from this work are given in Table 4. These measurements indicate that quadrupole interactions in metals can be determined rather accurately by PAC in cases for which the extranuclear environment is unique and unambiguous.

3. Magnetic Resonance Detected by Angular Correlations.--

In 1953 Abragam and Pound (6) suggested that the precision of NMR could be combined with the sensitivity of PAC if magnetic resonance in the intermediate state could be detected by applying a radiofrequency field and detecting its effect, when the resonance condition was satisfied, on the angular correlation. Thus instead of observing the time development of $G_{\lambda',\lambda}^{q',q}(t)$ under "free precession" conditions, the resonance would be driven. Two detectors could be placed at suitable angles and a time-integral coincidence rate measured as a function of the frequency of the applied field. Experiments of this kind have been carried out on ^{100}Rh nuclei in ferromagnetic lattices of nickel (28) and iron (29). Although a complete theory for this kind of resonance experiment has been given (10), it is instructive to describe it in

Table 4. Quadrupole Coupling Constants in Metals from PAC (Ref. 27)

Parent	Daughter	Intermediate State Energy (keV)	Spin	$e^2qQ(MHz)$[a] in					
				Tl	Hg	Cd	In	Zn	Sn
$^{111}Cd^m$	^{111}Cd	247	5/2	20.8(8)	110(1)	125(2)	17.3(3)		
^{111}In	^{111}Cd	247	5/2		112(1)	126(1)	17.3(2)	123(1)	24.2(3)
$^{204}Pb^m$	^{204}Pb	1274	4	13.4(3)	129[b]	118(6)	41(1)		71.2(15)
^{99}Rh	^{99}Ru	99	3/2			24.2(6)		21(1)	24.0(15)

[a]Errors in last digit are given parenthetically.

[b]Inhomogeneously broadened.

simple physical terms. Let us consider the correlation of two dipole transitions that connect a three-level system with spins in the sequence 0, 1, 0. A magnetic field $\vec{H}_o$ is applied, incurring an effective field $\vec{H}'_o$ at the nuclei, and splitting the intermediate states into three substates with M = 1, 0, and -1, spaced in energy by $g\mu_N A'_o$, where g is the intermediate-state g factor. For maximum sensitivity $\vec{k}_1$ and $\vec{k}_2$ are taken parallel and antiparallel to $\vec{H}_o$. The γ-ray transitions have two different kinds of components, the σ, or $\Delta M = \pm 1$ components, and the π components, with $\Delta M = 0$. Because their angular distributions go as $1 + \cos^2\theta$ and as $\sin^2\theta$ respectively, the only substate sequences that can give coincidences in this geometry are

$$|I_i\rangle \xrightarrow{\sigma} |I, M = \pm 1\rangle \xrightarrow{\sigma} |I_f\rangle \text{ , or } (\sigma,\sigma) .$$

The sequence

$$|I_i\rangle \xrightarrow{\pi} |I, M = 0\rangle \xrightarrow{\pi} |I_f\rangle \text{ , or } (\pi,\pi) ,$$

cannot yield an observable coincidence, because neither photon will be detected. When a radiofrequency field $\vec{H}_1 = 2\vec{H}_1 \cos 2\pi\nu t$ is applied perpendicular to $\vec{H}_o$,

giving an effective oscillatory field $2\vec{H}_1'$ cos $2\pi\nu t$, and the resonance condition $h\nu = g\mu_N H_o'$ obtains, nuclei can undergo transitions from one magnetic substate to another while in the intermediate state. When this occurs, some of the would-be (σ,σ) sequences become (σ,π) sequences and are lost from the coincidence rate. Thus magnetic resonance appears as a decrease in the counting rate when $\nu = \nu_L$. In ^{100}Rh the spin sequence is actually 1, 2, 1, but the principle is the same (28).

Ferromagnetic lattices were used in the resonance experiments to take advantage of the "hyperfine enhancement" effect. It is difficult to apply a large enough H_1 field to induce resonance during the intermediate-state lifetime. To appreciate this we can consider the situation in the rotating frame at resonance. Under these conditions H_o is "transformed out", $\vec{H}_1(t)$ has become a steady field of strength H_1' along (e.g.) the x axis, and the torque equation governing the time-evolution of the system in this frame is (cf. Equations (8) and (9)):

$$\frac{d\vec{K}}{dt} = \frac{g\mu_N}{\hbar}\vec{K} \times H_1' \quad . \qquad 39.$$

The symmetry axis $\vec{K}$ therefore rotates about H_1' with angular frequency $\omega_1 = g\mu_N H_1'/\hbar$. For an appreciable fraction of the nuclei to undergo resonance it is therefore necessary that $\omega_1 \tau \sim 1$. Even in the very favorable case of ^{100}Rh, which has $g = 2.15$ and $\tau = 3 \times 10^{-7}$ sec, this would require a radio-frequency field strength of $H_1' = 300$ gauss. It would be impractical to apply such a field to the sample externally, but fortunately <u>any</u> applied field H_1 having a frequency much smaller than the ferromagnetic resonance frequency (which is in the 10^{10} Hz range) will polarize the conduction electrons adiabatically, creating a hyperfine field H_1' of the same frequency at the nuclei. This field is larger than H_1 by the hyperfine enhancement factor $f = H_{hf}/H_o$, which is usually in the range $10^2 - 10^3$. Thus a radiofrequency field of only ~ 1 gauss need be applied externally in the ^{100}Rh case.

It is instructive to follow the magnetic resonance work on ^{100}Rh in nickel, which is illustrated in Figure 6. The first observed resonance (28) was broad and asymmetric. Later observations under more carefully controlled conditions yielded a higher resonance frequency in the main component and resolved a doublet structure (29). Although the large linewidth was tentatively

attributed to relaxation effects, further work showed that the real cause was inhomogeneous broadening caused by a very small percentage of impurities in the sample (30). Such broadening is well-known in conventional NMR studies on ferromagnets (31). In a sample of higher purity a narrower line was observed at a slightly higher frequency than the higher-intensity component in the earlier work. The linewidth of this component was much smaller than before, and the satellite line, which was attributed to ^{100}Rh nuclei near impurities, was absent. Finally, improvements in fast-timing methods made it possible to study this case by the free-precession method. Both the fundamental Larmor frequency ν_L and the double frequency at $2\nu_L$ (cf. Equation (16)) were observed in the Fourier transform (cf. Equation (35)). Both the NMR experiments and the free precession studies can give resonant frequencies to a precision in the 0.1% region. It seems probable that both will be useful in studying subtle effects in dilute alloy systems.

4. Relaxation Studies in Metals.--

The experimental situation in this area is still rather tentative, and our comments here must be more in the nature of a progress report than a review.

Relaxation in metals is conveniently discussed in three parts, divided roughly according to the time domains in which the characteristic relaxation times fall.

The first category involves the well-known longitudinal and transverse relaxation times, T_1 and T_2, that are ordinarily associated with relaxation studies in metals by conventional NMR methods. These relaxation times tend to lie in the millisecond range, which is out of reach of most γ-γ correlation cascades, and therefore outside the scope of this article. This time range is ideally suited to in-beam studies, and a number of accelerator groups are currently studying relaxation times using closely-related angular-distribution techniques.

The second category includes the study of "transient fields" of 10^6 gauss or more experienced by ions injected into ferromagnetic metals. These fields arise through interactions between polarized conduction electrons and the nuclei of the ions as they are slowed down by electron scattering processes during their stopping times of $\sim 10^{-12}$ seconds. Transient fields lie outside the scope of this article as they involve in-beam, rather than γ-γ, correlations, and are more closely related to the stopping of heavy ions in solids than to properties of metals. Winther has recently discussed transient fields (32).

A third category of relaxation phenomena in metals lies between the above two extremes, and within the scope of this article. This category involves the usual relaxation times T_1 and T_2 for metals, but it includes cases in which the interactions are so strong as to bring these relaxation times down into the time range of $< 10^{-6}$ sec, where they are accessible to PAC studies. Unfortunately none of the cases studied to date can be interpreted in a completely unambiguous way, in the reviewers' opinion. The case that should be most nearly free of systematic error is that of ^{100}Rh in nickel near the Curie temperature. Rosenblum found time-dependent attenuation in time-differential PAC studies above T_c and has used parallel geometry ($\vec{H}_o \| \vec{k}_1$) to distinguish between relaxation and inhomogeneous broadening (33). He found that the characteristic relaxation constant λ_2 in $G_{22}(t)$ varies directly as σ^2, the square of the lattice magnetization. Reno and Hohenemser (34) found time-dependent attenuation below T_c. In both cases the effective fields at the nuclei are strongly temperature-dependent, and the attenuations could arise in part from temperature inhomogeneities.

Hershkind has recently summarized recoil and implantation results on rare earths in nonmagnetic metals (34). Integral PAC studies of a number of rare earths in copper, for example (35-37) show good agreement between the relative attenuations of the P_2 and P_4 terms and the predictions of a stochastic magnetic relaxation model by Blume (38). Time-differential studies, however, do not show such agreement (39,40). Since Blume's model is based on the assumption that the electronic spin is J = 1/2, whereas larger values of J are present in the rare earths, detailed agreement would not be expected. The present situation may be described by stating that magnetic relaxation is dominant in these cases, but more work is necessary before a quantitative description can be given. Blume's model treats the case $\omega_m \tau_c \sim 1$, where ω_m is the magnetic interaction strength and τ_c is the electronic correlation time, in contrast to the Abragam-Pound theory (6), which applies for $\omega_m \tau_c << 1$. Thus Blume's approach might be expected to work after modifications to account for larger J values.

Finally, Bernas and Gabriel (41) have considered relaxation of ^{169}Tm in the iron lattice. By studying integral correlations in two states with lifetimes

differing by a factor of 5 they were able to deduce a relaxation time constant of 5 psec for this case.

B. Angular Correlations in Insulators

The experimental situation for PAC in insulators is in a much more primitive state than in metals. Referring to the second "layer" of Figure 4, we can immediately eliminate three of the four columns. No resonance-PAC work in insulators has been reported. Although PAC patterns in insulators frequently show attenuation, this can probably be attributed to inhomogeneous broadening effects in most cases. Magnetic perturbations are undoubtedly present in some insulators that have been studied, but very little effort has been directed toward studies of magnetic perturbations because most workers have preferred to study magnetic ions in solution, thereby eliminating the additional problems associated with the crystal lattice. This leaves quadrupole interactions as the only topic sufficiently well studied in insulators by PAC techniques to warrant review at this time.

Even quadrupole interactions have not given very promising results in many cases. In their 1965 review article (7) Frauenfelder discussed only two cases

in which time-differential studies on insulators were analyzed in detail. A very careful study of the 482-keV, I = 5/2 state of ^{181}Ta in single crystals of NH_4HfF_6 was reported by Mayer, et al. (42). They used ^{181}Hf as a parent, so the γ-γ cascade followed β^--decay. Several oscillations were observed. The other case discussed by Frauenfelder and Steffen was the work of Lehmann Miller (24) on ^{111}Cd produced by the electron-capture decay of ^{111}In in In_2O_3 and $In(OH)_3$. In both cases $G_{22}(t)$ is largest (presumably near unity) at t = 0. It drops quickly to zero, then rises to a small positive value. This behavior can be explained at least qualitatively as arising from static perturbation by a distribution of quadrupole frequencies (7,43). Several other studies of quadrupole perturbations by PAC were cited (7). The results were both tantalizing and discouraging. Oscillations could be observed in some cases, but in other cases the results were ambiguous. Effects of preceding decays appeared to be very important, and these effects were discussed by Frauenfelder and Steffen. The reviewers have recently made PAC studies of a large number of compounds to help clarify this question (27). The results are summarized below.

1. Correlations Following Isomeric Decay.--

When γ-γ cascades fed by the isomeric decays of $^{111}Cd^{m}$, $^{204}Pb^{m}$, and $^{199}Hg^{m}$ were studied in a total of 41 lattices, no effects attributable to the perturbation of the atomic environment were observed. This was expected, because the recoil energies in these isomeric transitions are less than 1 eV. In most cases $G_{22}(t)$ was well enough defined to yield quadrupole coupling constants. Attenuation over the relatively long time scale of 10^2 - 10^3 nsec was observed in some cases. The conclusion was drawn that the derived interaction constants are representative for the sites occupied by the isomeric nuclei before decay. Since these isomeric states are sufficiently long-lived to permit chemical synthesis it follows that PAC methods are generally applicable to compounds of Cd, Pb, and Hg. The time-differential PAC spectrum for a typical case--$^{111}Cd^{m}$ in $CdCl_2$--is shown in Fig. 7.

Correlations Following Beta Emission.--

When a nucleus undergoes $\beta^{\pm}$ decay, the nuclear charge suddenly changes by one unit, and the electrons in bound orbitals may or may not be able to follow adiabatically. Experiments on free atoms have established that about

80% of the daughter atoms have a charge of +1 following β^- decay, with the rest in higher charge states (44,45). This augers well for angular correlation studies following beta decay. The majority of daughter atoms should have the same number of electrons as the parent, for any given sample. Thus the daughter's oxidation state will be higher by one for β^- decay, and lower by one for β^+ decay. In most cases the angular correlation is carried out on a stable species, but one that is rather unusual in being a daughter impurity atom in a lattice compound of the parent element.

Experiments in ^{111}Cd and ^{181}Ta following the β^--decay of ^{111}Ag and ^{181}Hf in a total of 14 insulating materials have shown that a well-defined field gradient exists in 80-90% of the daughter sites (27). Figure 7 shows data for ^{111}Ag in Ag_2SO_4. This agrees with the early work (42) on ^{181}Hf in NH_4HfF_6 and other cases. It appears to be rather well established that quadrupole coupling constants can be determined by PAC following β^- decay in insulators. No conclusions about β^+ decay can be drawn as yet because of lack of data.

Correlations Following Electron-Capture Decay.--

After an electron is captured from the K shell, a number of processes take place on increasing time scales. The K hole is usually filled radiatively in 10^{-15} sec or less for elements of interest here. As the hole moves out further, Auger effects become dominant, with the creation of more holes. In 10^{-14} sec or less these holes will have migrated to the outermost shell where, in an insulator environment, they can survive for times that are long compared to the nuclear intermediate-state lifetime. The PAC experiment will therefore be performed in a sample in which the atoms are in several highly-charged states. Under these conditions the perturbation factor would be severely affected. In fact for all electron capture experiments in insulators using ^{99}Rh, ^{100}Pd, and ^{111}In as parents, remarkably similar behavior was observed (27). The anisotropy was strongly attenuated in a short time and no periodic behavior was found. Obviously the study of quadrupole coupling in insulators by PAC following electron-capture decay is strongly influenced by this effect, and great caution is necessary in the interpretation of experimental data. Data for ^{111}In in $InPO_4$ are shown in Fig. 7.

C. Angular Correlations in Solutions

The word "solutions" rather than "liquids" appears in the title of this section for two reasons. First, nearly all of the experimental work in this area to date has in fact involved solutions. Second, in studies of large molecules in solutions or of high viscosity solutions (including glasses), local molecular properties are more important than is the fact that the environment is at least technically a liquid.

Referring to Figure 4, we are now interested in the third layer of 4 × 4 "boxes". The considerations regarding mode of decay are essentially the same as for solids, and further systematic discussion is unnecessary. Due to the molecular motion, charge equilibrium is reached much faster than in insulators, however. No resonance experiments have been carried out as yet in solutions. The three remaining categories are relaxation, quadrupole coupling, and magnetic coupling. In most solution studies relaxation is an important, or even a dominant, process. This is especially true for magnetic coupling, in the cases studied thus far: relaxation is so fast that magnetic properties of the ions under study appear as paramagnetic shifts modifying the applied magnetic fields. This topic is discussed first below. Quadrupole interactions have been studied in solutions

for situations ranging from the very fast relaxation limit to cases in which relaxation was imperceptibly slow. This whole range is discussed in Section C.2.

1. Magnetic Interactions in Solutions.--

Most of the early PAC work on excited-state nuclear moments involved ions in solutions and the application of external magnetic fields. To minimize chemical effects in the intermediate state, strongly acidic solutions were employed. In the case of beta decay to an ion with a closed-shell configuration the effective magnetic field at the nuclei $\vec{H}_e$ would most likely be equal to the applied field $\vec{H}_o$, and reliable interpretations were possible. In the case of paramagnetic ions, paramagnetic corrections were necessary. These could be described by a "paramagnetic factor", β. Thus

$$\vec{H}_e = \beta \vec{H}_o \quad . \qquad 40.$$

The factor β would be rather difficult to estimate in general, because of an inexact knowledge of the daughter atomic electron configuration. In rare earths the β factors are very large (up to 7 or 8 at room temperature), and

they may be estimated in a straightforward way. The electronic level is assumed to be polarized and in rapid equilibrium. This gives

$$\beta = H_N(\langle J_z \rangle/J) - 1 \qquad 41.$$

where H_N is the field at the nucleus when the electronic level is completely polarized in the $M_J = J$ state. The mean value $\langle J_z \rangle$ is given by a Brillouin function involving the Zeeman and thermal energies. Of course this approach presupposes that the electronic configuration is both unique and known. This isn't quite true even for beta decay, as discussed in Section B, and even less so in the case of electron capture. Matthias, et al. (18) discussed the specific case of ^{99}Ru in a chloride solution and concluded that an error of ± 10% should be associated with the estimate of β. For most other cases studied to date the error is probably fully this large. Thus paramagnetic ions in aqueous solutions are suitable for measuring nuclear g-factors to ∿ 10% accuracy, and it may also be of interest to determine which oxidation states are present after beta or electron-capture decay by studying $G_{22}(t)$ in solutions. At present, however, it does not appear feasible to study subtler properties with such poorly-characterized samples.

2. Quadrupole Interactions in Solutions.--

Most of the work in this area has been done on ions in the limit $\omega_Q \tau_c << 1$, where ω_Q is a characteristic quadrupole frequency and τ_c is a correlation time describing the fluctuation rate of transient field gradients that cause relaxation in the intermediate state. In this limit Abragam and Pound (6) gave the simple expression for the perturbation coefficient

$$G_{\lambda\lambda}(t) = e^{-k_\lambda t} \quad . \qquad 42.$$

When relaxation arises from axially-symmetric field gradients V_{zz}, k_λ has the form (6,7)

$$k_\lambda = \frac{3\tau_c}{80} \left(\frac{eQ}{h}\right)^2 \langle V_{zz}^2 \rangle \frac{\lambda(\lambda+1)[4I(I+1) - \lambda(\lambda+1) - 1]}{I^2(2I-1)^2} \quad , \qquad 43.$$

where $\langle V_{zz}^2 \rangle$ denotes an ensemble average. The time-integrated perturbation factor is given by

$$G_{\lambda\lambda}(\infty) = \frac{1}{1 + k_\lambda \tau} \quad , \qquad 44.$$

where τ is the nuclear lifetime. Early experiments (46-48) on the ^{111}Cd cascade showed that Equations (42) - (44) appear to describe quadrupole relaxation quite

well. The correlation times were varied in these studies by varying the viscosity of the solutions.

Quadrupole relaxation has found surprisingly few applications as yet. Recently, however, the Bonn group has applied this phenomenon to the measurement of the nuclear relaxation times in solutions. They have also derived quadrupole-moment ratios from relaxation constants (50,51). In ^{172}Yb they found the ratio of the quadrupole moments of the 1172-keV 3+ state to that of the 78-keV 2+ state to be 1.32 ± 0.14, in excellent agreement with the value 1.33 ± 0.15 as measured by a "conventional" PAC experiment (52).

Another recent application of PAC to solutions is the use of "rotational tracers" to follow the dynamical behavior of molecules in solution. The first work in this area (53) employed the γ-ray cascade in ^{111}Cd following the decay of $^{111}In^{3+}$ bound to active sites in bovine serum albumin (BSA). The $G_{22}(t)$ function was found to be sensitive to denaturation of BSA in a way that is consistent with the correlation time decreasing as the molecule became less rigid. Because of the uncertainties associated with electron-capture decay of ^{111}In, it was also desirable to use the isomeric $^{111}Cd^{m}$ state as the parent

nucleus. Meares, et al. (54) showed that $(^{111}Cd^{m})^{2+}$ binds into the Zn^{2+} position in carbonic anhydrase. The $G_{22}(t)$ function for this case resembled that of a polycrystalline sample, indicating that the Cd^{2+} site was essentially "immobilized" in this large molecule. For samples of $(^{111}Cd^{m})^{2+}$ bound to N-benzyliminodiacetic acid a strong temperature-dependence of the attenuation constant k_2 was observed. The $G_{22}(t)$ functions studied ranged from a "polycrystalline" appearance at 77°K to fast relaxation with a correlation time $\tau_c \cong 10^{-10}$ sec at 356°K (55). Similar results have been obtained with ^{181}Ta in ice (56) and with ^{111}In in frozen solutions of $InCl_3$ and $In(NO_3)_3$ (57). In each case the time-integrated coefficient $G_{22}(\infty)$ had the value unity for correlation times so short that the condition $\omega_Q\tau_c \ll 1$ was fulfilled. As τ_c increased, $G_{22}(\infty)$ decreased to a value of ≈ 0.1 in the region $\omega_Q\tau_c \sim 1$, and for long correlation times $G_{22}(\infty)$ increased to approximately the expected (7) "hard-core" value of 1/5. The expected variation of $G_{22}(\infty)$ with τ_c is therefore qualitatively well-established, albeit on samples in which neither the site symmetry nor the actual magnitude of e^2Qq is well characterized. It will be interesting to learn whether quantitative agreement with calculations based on

a slow rotational diffusion model (58,59) will be realized when better-characterized samples are studied. A good candidate for such experiments in dimethylcadmium, which maintains its molecular integrity in frozen solutions. A time spectrum for the case of dimethyl-$^{111}Cd^{m}$ in a frozen ether solution (27) is shown in Fig. 8. The PAC technique is a natural choice for studying rotation motion in liquids. With improvements in technique and interpretation, it may have more future applications in this area.

D. Angular Correlations in Gases

Relatively little PAC work of other than nuclear interest has been done on gases. Except for extremely short-lived states, experiments on gaseous samples to date have been carried out under fast or intermediate relaxation conditions. That is, $\omega\tau_c$ was either much less than unity or of the order of unity. Here ω is a magnetic or quadrupole hyperfine frequency and τ_c is a correlation time. Since relaxation in gases arises from molecular collisions, which are in most cases sufficiently violent events to randomize the molecular orientation, τ_c is expected to be of the same order of magnitude as the collision time.

Time-dependent magnetic interactions have been observed in ions recoiling into gases following nuclear reactions or decay. The ions are typically in rather high charge states, of the order + 10. Consequently, magnetic interactions are present that can be characterized by effective magnetic fields of $\sim 10^8$ gauss, created mainly by the Fermi contact interaction with unpaired s electrons. The main motivation for studying these systems is their use in determining magnetic moments of very short-lived nuclear states with lifetimes in the picosecond range. Most of the measurements to date have been of the time-integral variety, but time-of-flight methods have recently been used to obtain more definitive time-differential data (60,61), and there is already evidence that favors intermediate relaxation conditions ($\omega\tau_c \sim 1$) over fast relaxation ($\omega\tau_c \ll 1$). Goldring (62) and Sprouse (63) have summarized this area of research in recent review articles.

Finally, time-differential gas phase PAC studies of the γ-ray cascade in ^{111}Cd following the decay of ^{111}Cd^m in dimethylcadmium have been carried out in the presence of various buffer gases at 1.5 atm. (27). The ^{111}Cd nucleus has a well-defined environment, with the field gradient projected along the molecular rotation axis being related to that in the molecular frame by

$$q_{eff} = -q_{mol}/2 \quad . \qquad 45.$$

Strong attenuations were observed in all ten cases studied, with λ_2 ranging from 10 to 45 $(nsec)^{-1}$. For heavy buffer gases a strong-collision model is appropriate, with the values of τ_c deduced on this model being essentially equal to the characteristic collision time τ_{coll}. Very light molecules (H_2 and He) did not follow this trend, however: for these cases τ_c was found to exceed τ_{coll}. This was interpreted as showing that the impact of these small molecules is too small to randomize the rotation axis of a dimethylcadmium molecule in a single collision. Typical results are given in Table 5.

E. Summary

The theory of γ-ray angular correlations is essentially a closed subject, so only the experimental situation needs summarizing.

In the seven years since the 1965 review article of Frauenfelder and Steffen appeared, time-differential PAC has developed as a tool that is now sufficiently well-understood and precise to find applications in studies of the extranuclear environment. In metallic samples PAC is a proved method that can compete with other established techniques. It has been used for studies of

Table 5. Correlation times for dimethylcadmium in buffer gases at 1.5 atm. (Ref. 27)

Gas	λ_2^{-1}(nsec)	τ_c(nsec)	τ_{coll}(nsec)
H_2	10 ± 3	0.17	0.017
He	20 4	0.09	0.026
N_2	36 5	0.05	0.051
Ar	30 5	0.06	0.061
Xe	26 4	0.07	0.082

hyperfine fields, Knight shifts, and quadrupole interactions. Characteristic lines have been obtained both by magnetic resonance and by Fourier analysis of time-differential perturbation coefficients. Only relaxation phenomenon in metals have yet to be fully explored. This rapid progress is mainly due to the first equilibration of charge states by conduction electrons in metals. No such advances can be expected in other materials, except for γ-ray cascades following the decay of isomeric states. In insulating solids, static quadrupole interactions have been well-characterized following isomeric decay and beta decay, but not electron-capture decay. In solutions and gases angular-correlation studies usually involve relaxation phenomena, although more structure in $G_{22}(t)$ has been observed in macromolecules and frozen solutions. Further progress in the near future will probably involve applications of PAC to problems involving metals, and development of more sophistication in relaxation studies using solid, liquid, and gaseous samples.

LITERATURE CITED

1. Hamilton, D. R. 1940. Phys. Rev. 58:122

2. Brady, E. L., Deutsch, M. 1947. Phys. Rev. 72:870

3. Goertzel, G. 1946. Phys. Rev. 70:897

4. Frauenfelder, H. 1951. Phys. Rev. 82:549; Aeppli, H., Bishop, A. S., Frauenfelder, H., Walter, M., and Zünti, W. 1951. Phys. Rev. 82:550

5. Alder, K. 1952. Helv. Phys. Acta. 25:235; Alder, K., Albers-Schönberg, H., Heer, E., and Novey, T. B. 1953. Helv. Phys. Acta. 26:761

6. Abragam, A., Pound, R. V. 1953. Phys. Rev. 92:943

7. Frauenfelder, H., Steffen, R. M. 1965. Alpha-, Beta-, and Gamma-Ray Spectroscopy, ed. K. Siegbahn, Vol. 2:997. North-Holland.

8. The conditions are: $\lambda' \leqslant$ (the smaller of 2I or 2L') and $|I - I_i| \leqslant L' \leqslant |I + I_i|$.

9. Condon, E. U., Shortley, G. H. 1935. Theory of Atomic Spectra, Chapter IV. Cambridge University Press.

10. Matthias, E., Olsen, B., Shirley, D. A., Templeton, J. E., Steffen, R. M. 1971. Phys. Rev. A4:1626

11. Raghavan, R. S., Raghavan, P., Sperr, P. 1971. Hyperfine Interactions in Excited Nuclei, ed. G. Goldring and R. Kalish, Vol. 2-462. Gordon and Breach.

12. Matthias, E., Rosenblum, S. S., Shirley, D. A. 1965. Phys. Rev. Letters 14:46

13. The density-matrix notation of Reference 10 is used here.

14. This is the most common definition. There are several conventions in use, and original sources should always be consulted.

15. Note that the system must recover faster than the lifetime of the initial state, not that of the intermediate state.

16. Matthias, E. Lindquist, T. 1961. Nucl. Instr. Methods 13:356

17. Hrynkiewicz, A. Z. 1962. Nucl. Instr. Methods 16:317

18. Matthias, E., Rosenblum, S. S., Shirley, D. A. 1965. Phys. Rev. 139:B532

19. Matthias, E., Shirley, D. A. 1966. Nucl. Instr. Methods 45:309

20. Rao, G. N., Matthias, E., Shirley, D. A. 1969. Phys. Rev. 184:325

21. Alonso, J., Grodzins, L. 1968. Hyperfine Structure and Nuclear Radiations, ed. E. Matthias and D. A. Shirley, p. 549. North-Holland.

22. Shirley, D. A., Rosenblum, S. S., Matthias, E. 1968. Phys. Rev. 170:363

23. Reno, R. C., Hohenemser, C. 1970. Phys. Rev. Letters 25:1007

24. Lehmann, P., Miller, J. 1955. Compt. rend. 240:248; 1956. J. phys. radium 17:526

25. Raghavan, P., Raghavan, R. S. 1971. Phys. Rev. Letters 27:724

26. Raghavan, R. S., Raghavan, P. 1972. Phys. Rev. Letters 28:54

27. Haas, H., Shirley, D. A., submitted to J. Chem. Phys.

28. Matthias, E., Shirley, D. A., Klein, M. P., Edelstein, N. E. 1966. Phys. Rev. Letters 16:974

29. Matthias, E., Shirley, D. A., Edelstein, N., Körner, H. J. 1968. Hyperfine Structure and Nuclear Radiations, ed. E. Matthias and D. A. Shirley, p. 878. North-Holland.

30. Koički, S., Koster, T. A., Pollak, P., Quitmann, D., Shirley, D. A. 1970. Phys. Letters 32B:351

31. Budnick, J. I., Burch, T. J., Skalski, S., Raj, K. 1970. Phys. Rev. Letters 24:511

32. Winther, A. 1971. Hyperfine Interactions in Excited Nuclei, ed. G. Goldring and R. Kalish, Vol. 4-1055. Gordon and Breach.

33. Rosenblum, S. S. 1969. Ph.D. Thesis, University of California Lawrence Berkeley Laboratory Report UCRL-18675, unpublished.

34. Hershkind, B. 1971. Hyperfine Interactions in Excited Nuclei, ed. G. Goldring and R. Kalish, Vol. 4-987. Gordon and Breach.

35. Waddington, J. C. et al 1970. Nuclear Reactions Induced by Heavy Ions, p. 367. North-Holland.

36. Gilad, P., Goldring, G., Herber, R., Kalish, R. 1967. Nucl. Phys. A91:85

37. Skaali, B., Günther, C., Hershkind, B., Ravn, H. 1970. Presented at the International Conference on Angular Correlations, Delft.

38. Blume, M. 1968. Hyperfine Structure and Nuclear Radiations, ed E. Matthias and D. A. Shirley, p. 911. North-Holland.

39. Heestand, G. M. et al 1970. Presented at the International Conference on Angular Correlations, Delft.

40. Ryge, P., Kugel, H. W., Borchers, R. R. 1971. Hyperfine Interactions in Excited Nuclei, ed. G. Goldring and R. Kalish, p. 1043. Gordon and Breach.

41. Bernas, H., Gabriel, H. 1971. Hyperfine Interactions in Excited Nuclei, ed. G. Goldring and R. Kalish, p. 221. Gordon and Breach.

42. Mayer, L., Bodenstedt, E., Günther, C. 1964. Z. Physik 177:28

43. Matthias, E., Schneider, W., Steffen, R. M. 1963. Phys. Letters 4:41

44. Snell, A. H., Pleasanton, F. 1957. Phys. Rev. 107:740

45. Carlson, T. A. 1963. Phys. Rev. 130:2361

46. Hemmig, P. B., Steffen, R. M. 1963. Phys. Rev. 92:832

47. Albers-Schönberg, H., Heer, E., Scherrer, P. 1954. Helv. Phys. Acta. 27:637

48. Steffen, R. M. 1956. Phys. Rev. 103:116

49. Popp, M., Wagner, H. F. 1971. Hyperfine Interactions in Excited Nuclei, ed. G. Goldring and R. Kalish, Vol. 2-491. Gordon and Breach.

50. Forker, M., Wagner, H. F. 1969. Nucl. Phys. A138:13

51. Wagner, H. F., Forker, M. 1971. Hyperfine Interactions in Excited Nuclei, ed. G. Goldring and R. Kalish, Vol. 2-479. Gordon and Breach.

52. Li-Scholz, A., Rasera, R. L. 1969. Phys. Rev. Letters 23:181

53. Leipert, T. K., Baldeschwieler, J. D., Shirley, D. A. 1968. Nature 220:907

54. Meares, C. F., Bryant, R. G., Baldeschwieler, J. D., Shirley, D. A. 1969. Proc. Nat. Acad. Sci. 64:1155

55. Shirley, D. A. 1970. J. Chem. Phys. 53:465

56. Cameron, J. A., Gardner, P. R., Keszthelyi, L., Prestwich, V. V. 1969. Chem. Phys. Letters 4:229

57. Barrett, J. S. et al 1970. J. Chem. Phys. 53:759

58. Shirley, D. A. 1971. J. Chem. Phys. 55:1512

59. Marshall, A. G., Meares, C. F. 1972. J. Chem. Phys. 56:1226

60. Polga, T., Roney, W. M., Kugel, H. W., Borchers, R. R. 1971. Hyperfine Interactions in Excited Nuclei, ed. G. Goldring and R. Kalish, p. 961. Gordon and Breach.

61. Brenn, R., Lehmann, L., Spehl, H. 1971. Hyperfine Interactions in Excited Nuclei, ed. G. Goldring and R. Kalish, p. 966. Gordon and Breach.

62. Goldring, G. 1968. Hyperfine Structure and Nuclear Radiations, ed. E. Matthias and D. A. Shirley, p. 640. North-Holland.

63. Sprouse, G. D. 1971. Hyperfine Interactions in Excited Nuclei, ed. G. Goldring and R. Kalish, p. 931. Gordon and Breach.

FIGURE CAPTIONS

Fig. 1. The angular correlation function $W(\theta) = 1 + A_2P_2(\cos\theta) + A_4P_4(\cos\theta)$ for the typical case $A_2 = 0.3$, $A_4 = 0.2$. Here θ is the angle between the γ-ray propagations $\vec{k}_1$ and $\vec{k}_2$.

Fig. 2. Coordinate frame for magnetic perturbation experiments.

Fig. 3. Top panel: Decay curve of the 75-keV state of ^{100}Rh, measured by coincidence counting rate in the γ-ray cascade. The angles in the notation of Figure 2 are: $\theta_1 = \theta_2 = \pi_2$, $\phi_1 = 0$, $\phi_2 = \pm 3\pi/4$. Filled and open circles denote reversal of the applied field or (equivalently) change in the sign of ϕ_2. Bottom panel: Difference of the two data sets in the top panel divided by their sum, to isolate oscillatory modulation arising from Larmor precession.

Fig. 4. A scheme for categorizing PAC experiments.

Fig. 5. Temperature dependence of the field of a Cd nucleus in a Ni lattice, (a) below and (b) above the Curie temperature, after Reference 22. Solid curve in (a) gives lattice magnetization, while dashed curve represents a demagnetization correction. Solid curve in (b) was predicted from results in (a) using Equation (37).

Fig. 6. Resonance lines for ^{100}Rh in nickel. Panels (a) and (b) show NMR results from References 28 and 29, with some Pd impurity in the lattice. Panels (c) and (d) are, respectively, NMR and free precession results from Reference (30), with a high purity lattice. Lower frequency in (c) is attributed to radiofrequency heating.

Fig. 7. The function $A_2(t) \equiv \frac{2}{3}\,[W(\pi)/W(\frac{\pi}{2}) - 1] \cong A_{22}G_{22}(t)$, for three compounds, in which the 247-keV state of ^{111}Cd is populated following beta decay (Ag_2SO_4), isomeric decay ($CdCl_2$) and electron capture ($InPO_4$).

Fig. 8. The function $A_2(t)$ for $^{111}Cd^m$, in dimethyl-cadmium, in a frozen ether solution at 77°K. Inhomogeneous broadening is evident.

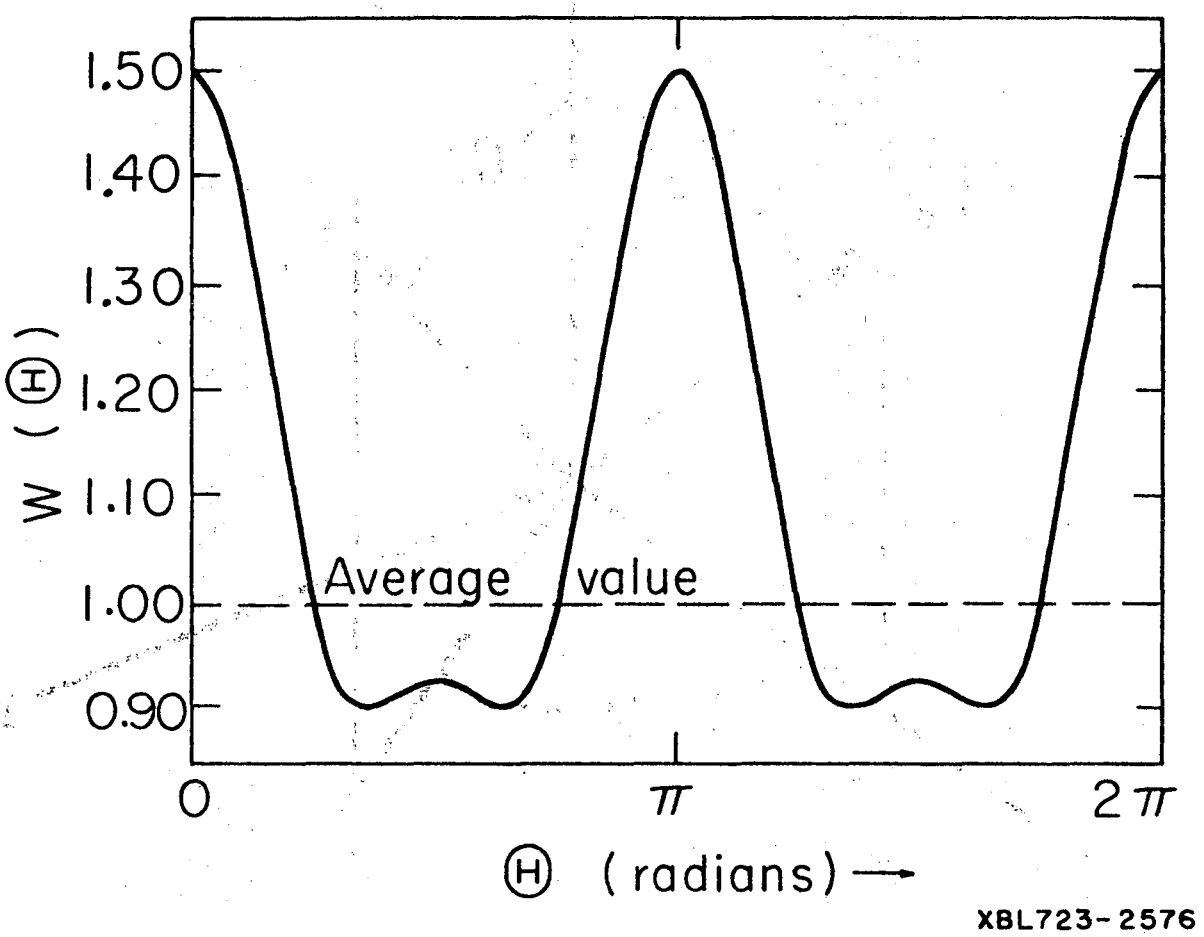

Fig. 1

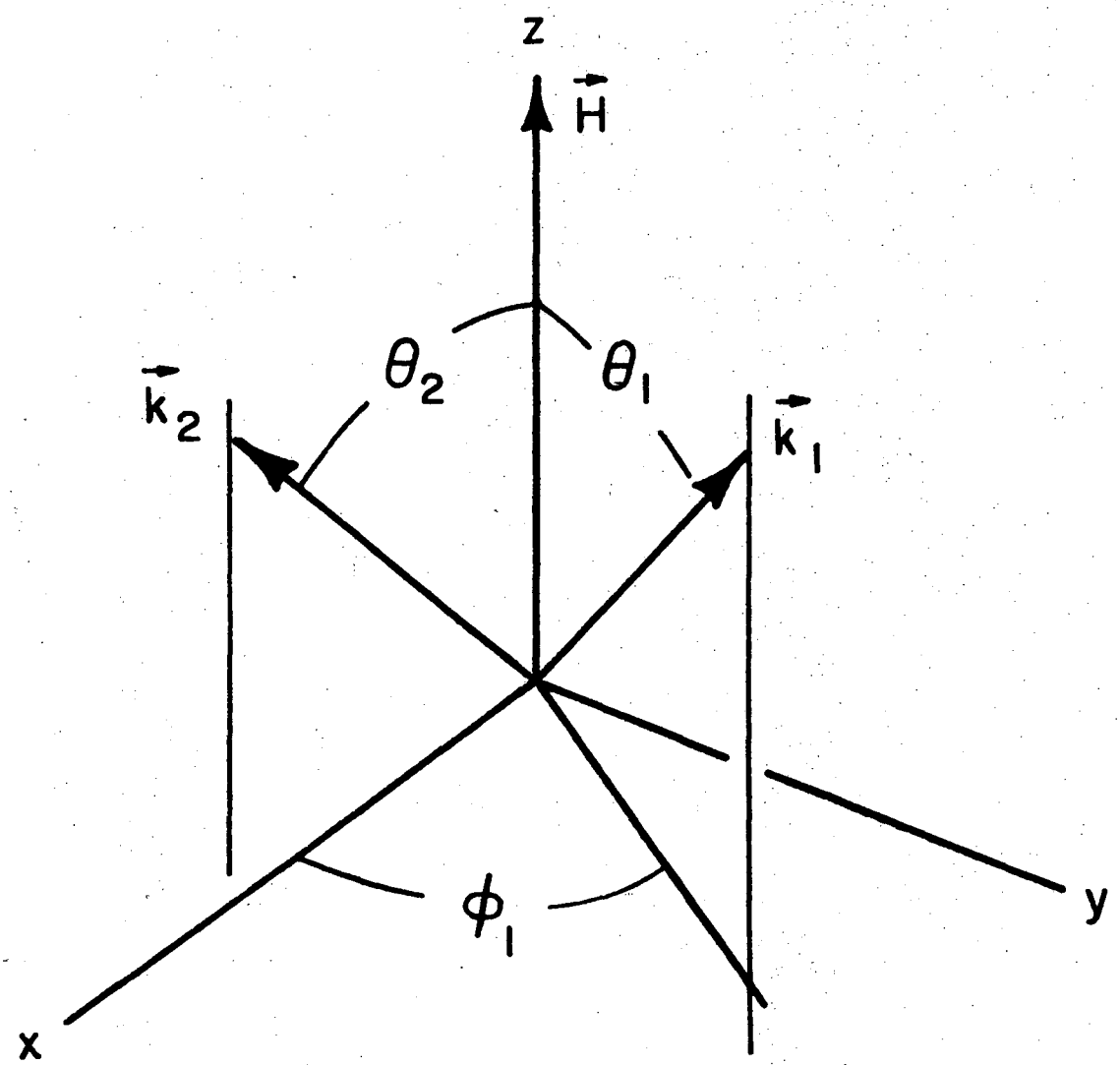

XBL723-2577

Fig. 2

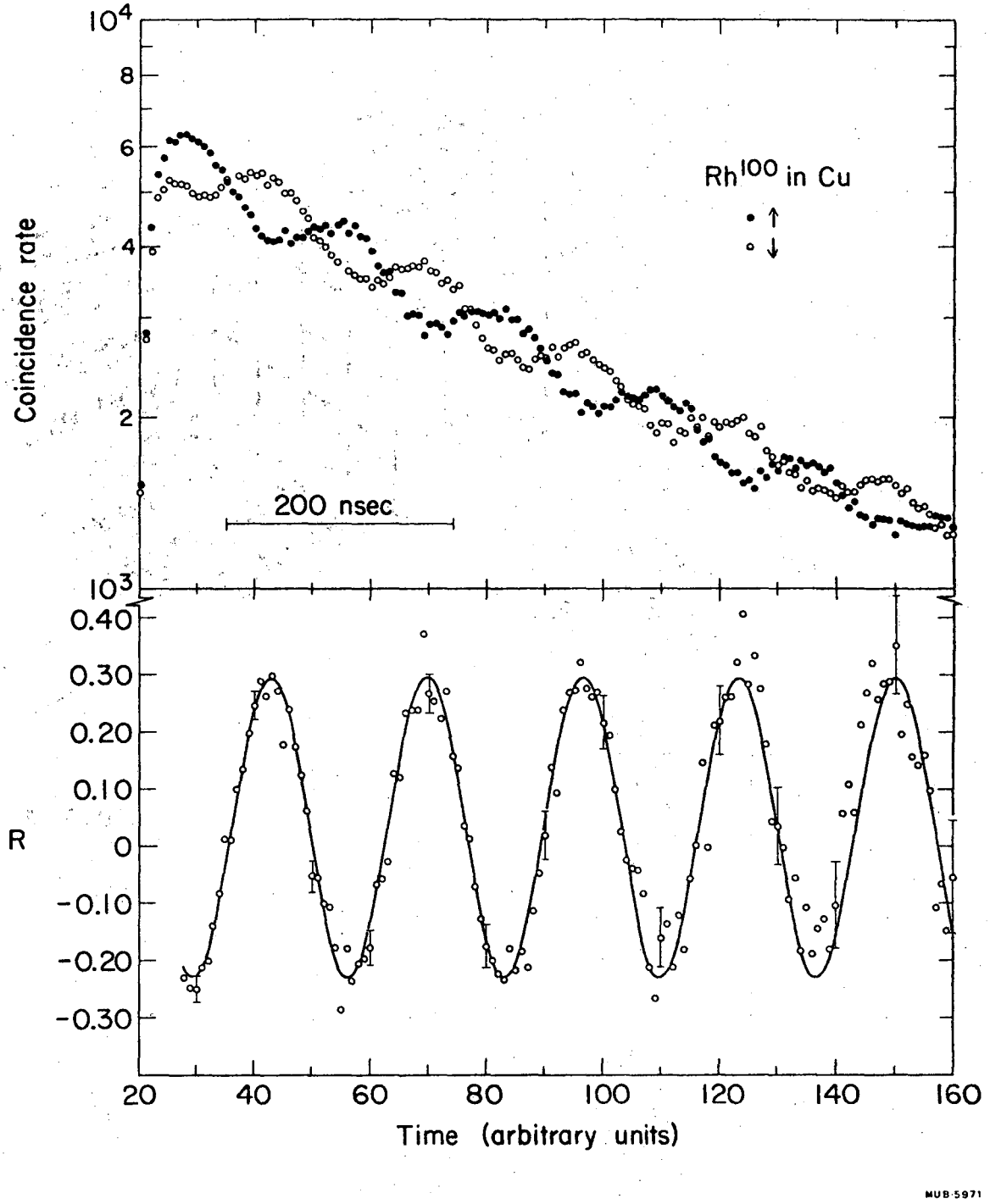
Coincidence rate
10^4
8
6
4
2
10^3
Rh^{100} in Cu
200 nsec
R
0.40
0.30
0.20
0.10
0
-0.10
-0.20
-0.30
20
40
60
80
100
120
140
160
Time (arbitrary units)
MUB-5971

Fig. 3

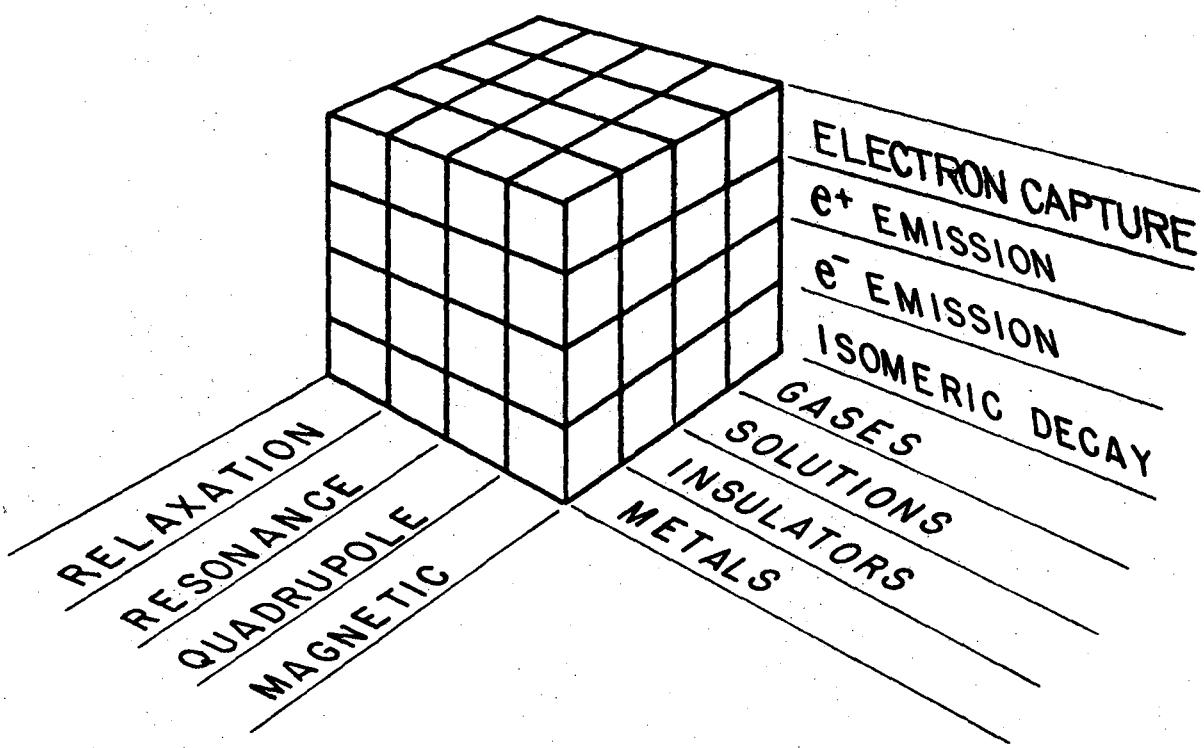

XBL723-2578

Fig. 4

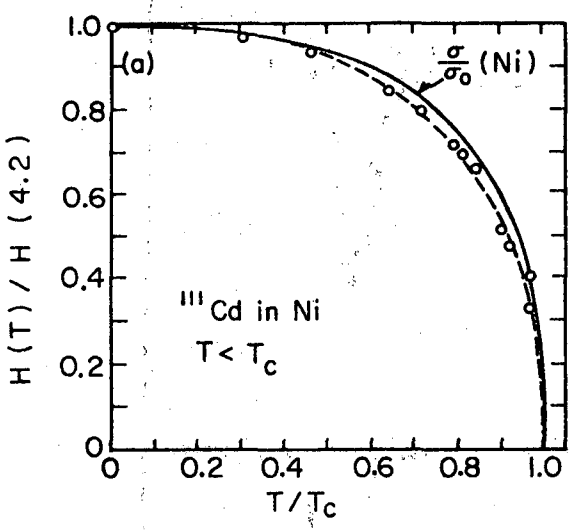

XBL723-2604

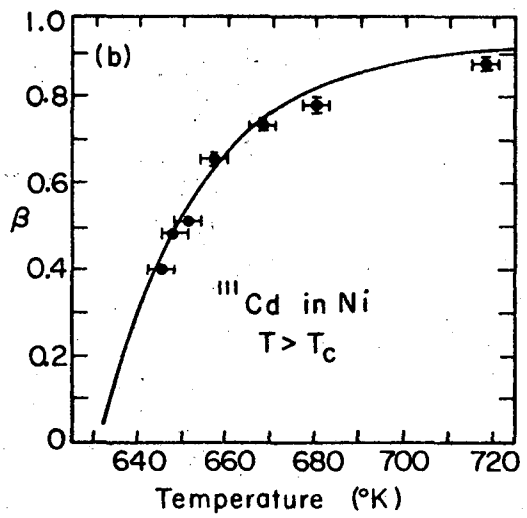

XBL723-2579

Fig. 5

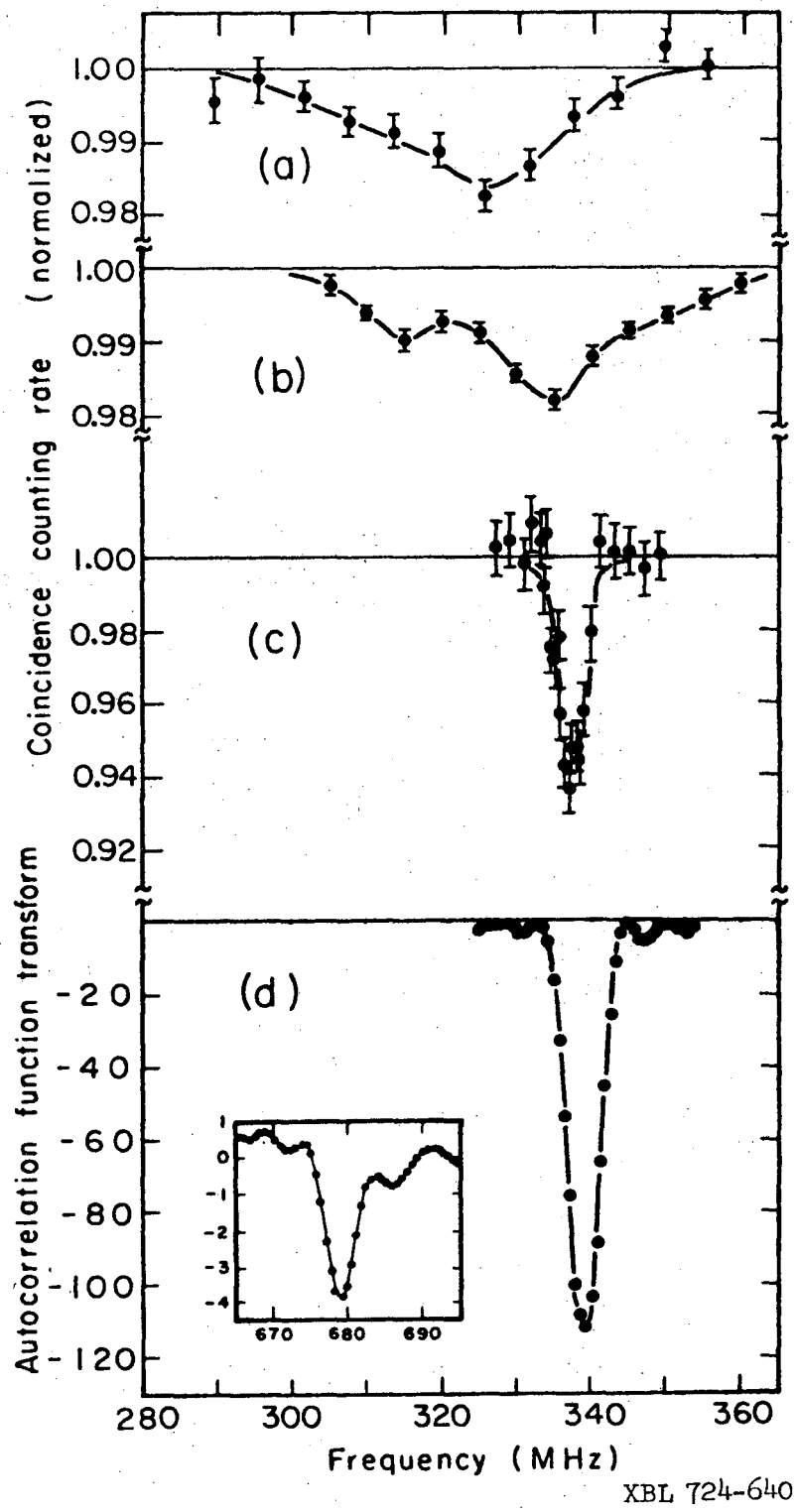
Coincidence counting rate (normalized)
1.00
0.99
0.98
(a)
1.00
0.99
0.98
(b)
1.00
0.98
0.96
0.94
0.92
(c)
Autocorrelation function transform
-20
-40
-60
-80
-100
-120
(d)
1
0
-1
-2
-3
-4
670
680
690
280
300
320
340
360
Frequency (MHz)
XBL 724-640

Fig. 6

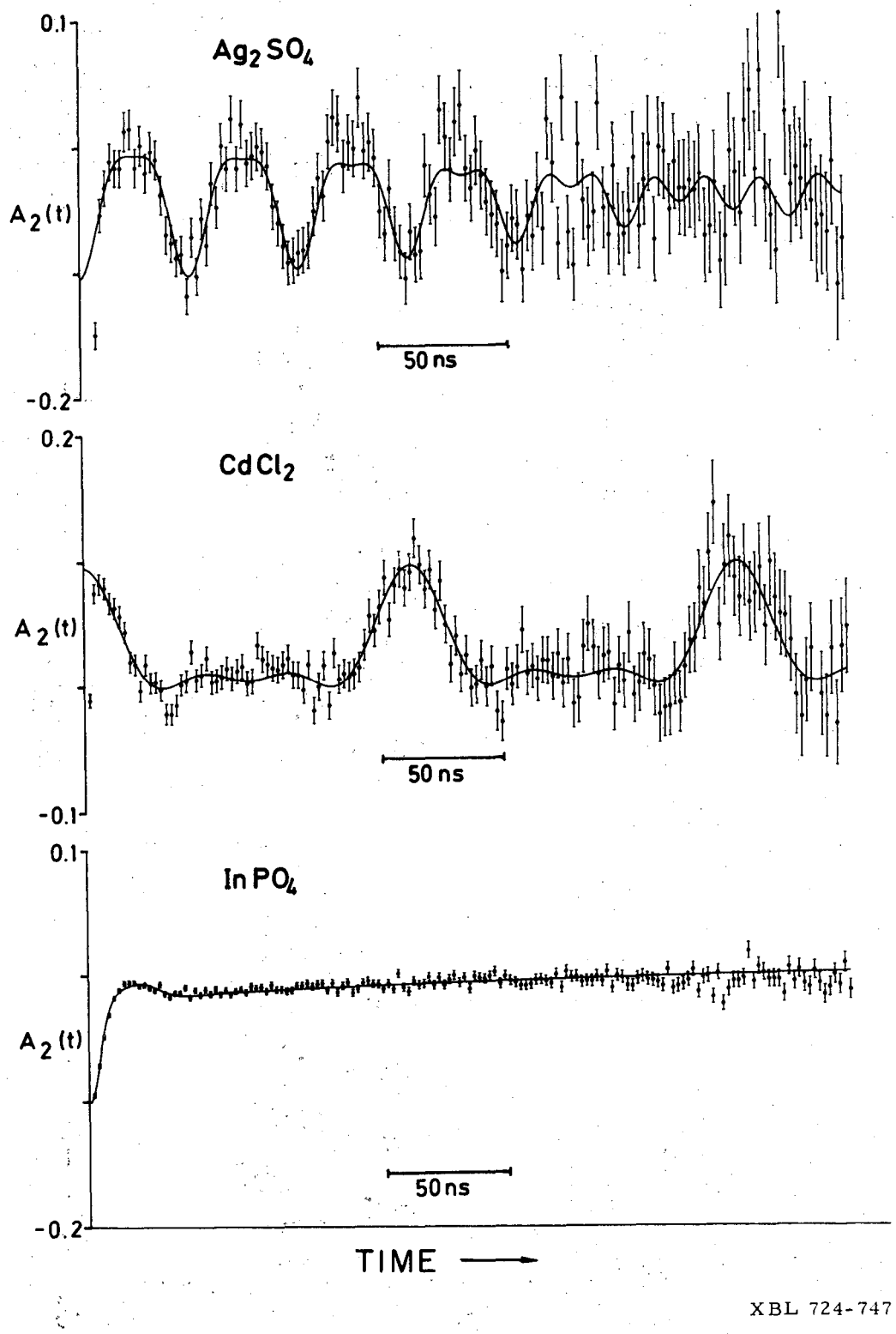
0.1
Ag_2SO_4
$A_2(t)$
-0.2
50 ns
0.2
$CdCl_2$
$A_2(t)$
-0.1
50 ns
0.1
$InPO_4$
$A_2(t)$
50 ns
-0.2
TIME
XBL 724-747

Fig. 7

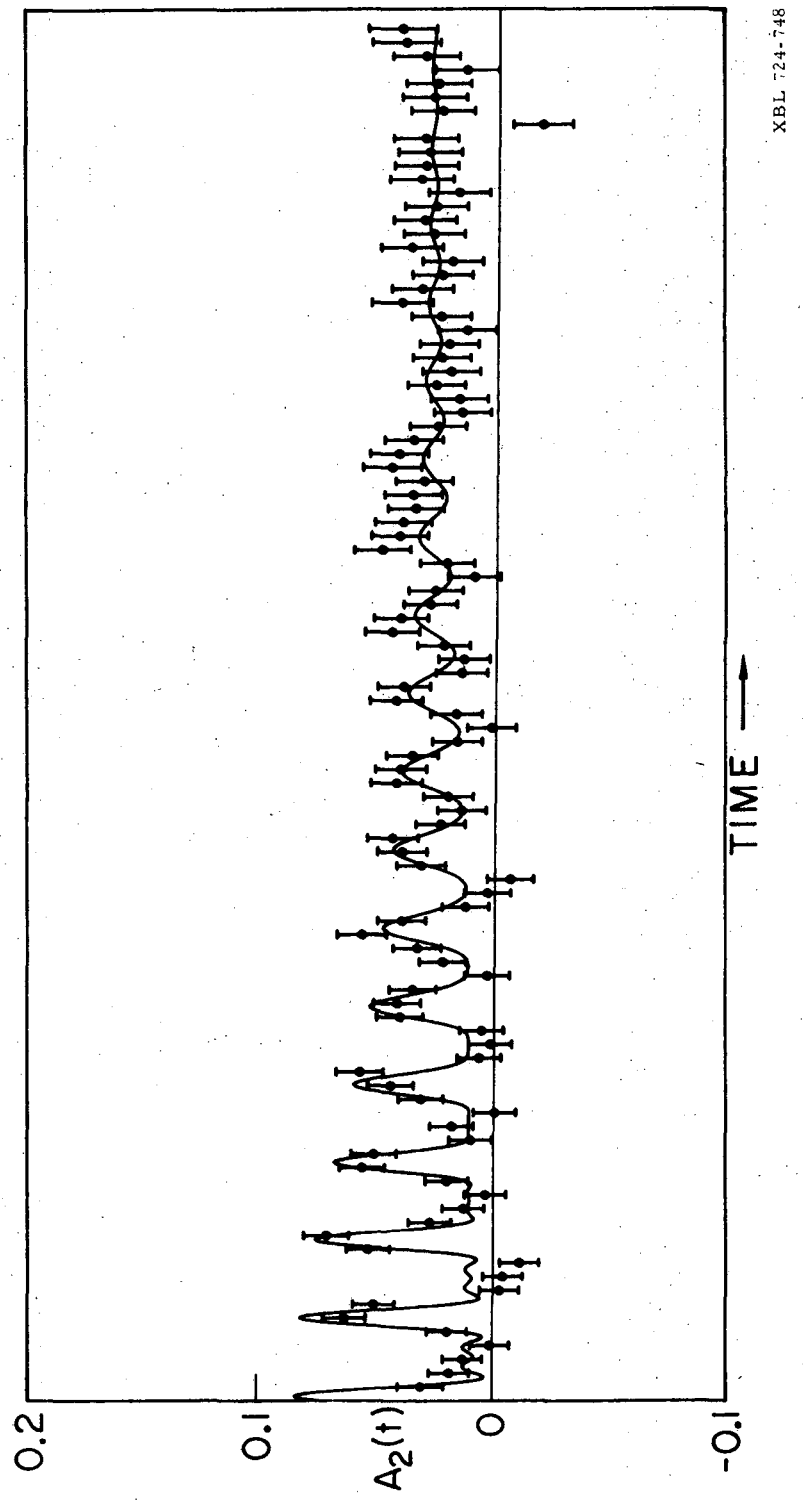

Fig. 8

TECHNICAL INFORMATION DIVISION
LAWRENCE BERKELEY LABORATORY
UNIVERSITY OF CALIFORNIA
BERKELEY, CALIFORNIA 94720